Plastic particles affect N_2O release via altering core microbial metabolisms in constructed wetlands

Yang, Xiangyu; Chen, Yi; Liu, Tao; Zhang, Lu; Wang, Hui; Chen, Mengli; He, Qiang; Liu, Gang; Ju, Feng

DOI
10.1016/j.watres.2024.121506

Publication date
2024

Document Version
Final published version

Published in
Water Research

Water Research 255 (2024) 121506

Contents lists available at ScienceDirect

Water Research

journal homepage: www.elsevier.com/locate/watres

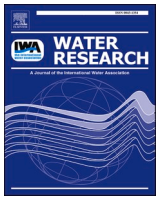

Plastic particles affect N_2O release via altering core microbial metabolisms in constructed wetlands

Xiangyu Yang [a,c,e,f,g], Yi Chen [a,b,*], Tao Liu [a,b], Lu Zhang [c,d], Hui Wang [c,d], Mengli Chen [a,b], Qiang He [a,b], Gang Liu [e,f], Feng Ju [c,d,**]

[a] Key Laboratory of the Three Gorges Region's Eco-Environment, Ministry of Education, College of Environment and Ecology, Chongqing University, Campus B, 83 Shabeijie, Shapingba, Chongqing 400044, China
[b] National Centre for International Research of Low-Carbon and Green Buildings, Chongqing University, Chongqing 400044, China
[c] Key Laboratory of Coastal Environment and Resources of Zhejiang Province, School of Engineering, Westlake University, 18 Shilongshan Road, Hangzhou 310024, China
[d] Institute of Advanced Technology, Westlake Institute for Advanced Study, 18 Shilongshan Road, Hangzhou 310024, China
[e] Key Laboratory of Drinking Water Science and Technology, Research Centre for Eco-Environmental Sciences, Chinese Academy of Sciences, Beijing 100085, China
[f] Department of Water Management, Faculty of Civil Engineering and Geosciences, Section of Sanitary Engineering, Delft University of Technology, Delft 2628 CN, the Netherlands
[g] Shandong Provincial Key Laboratory of Marine Environment and Geological Engineering, College of Environmental Science and Engineering, Ocean University of China, Qingdao 266100, China

ARTICLE INFO

Keywords:
Constructed wetlands
Plastic particles
Nitrous oxide
Nitrogen metabolism
Carbon metabolism

ABSTRACT

Constructed wetlands (CWs) have been proven to effectively immobilize plastic particles. However, little is known about the differences in the impact of varying sized plastic particles on nitrous oxide (N_2O) release, as well as the intervention mechanisms in CWs. Here, we built a lab-scale wetland model and introduced plastic particles of macro-, micro-, and nano-size at 100 μg/L for 370 days. The results showed that plastic particles of all sizes reduced N_2O release in CWs, with the degrees being the strongest for the Nano group, followed by Micro and Macro groups. Meanwhile, ^{15}N- and ^{18}O-tracing experiment revealed that the ammoxidation process contributed the most N_2O production, followed by denitrification. While for every N_2O-releasing process, the contributing proportion of N_2O in nitrification-coupled denitrification were most significantly cut down under exposing to macro-sized plastics and had an obvious increase in nitrifier denitrification in all groups, respectively. Finally, we revealed the three mechanism pathways of N_2O release reduction with macro-, micro-, and nano-sized plastics by impacting carbon assimilation (RubisCO activity), ammonia oxidation (gene *amo* abundance and HAO activity), and N-ion transmembrane and reductase activities, respectively. Our findings thus provided novel insights into the potential effects of plastic particles in CWs as an eco-technology.

1. Introduction

Plastic particles are an emerging plastic pollutant that is widely dispersed in various environments (Ivleva, 2021; MacLeo et al., 2021). Municipal wastewater treatment plants (WWTPs) are the primary sink and key point source of plastic particles entering natural water bodies (Xu et al., 2023; Simon et al., 2018). While most plastic particles in the wastewater influent (61–1189 μg/L) can be removed from final effluent (0.5–11.9 μg/L), these persistent pollutants pose a serious threat to biosafety due to their sizes (macro- or micro-sized plastics: 1000 nm < φ < 5 mm, nano-sized plastics: φ < 1000 nm) characteristics and physicochemical properties (Koelmans et al., 2022). Particularly, in terms of migration trends in wastewater treatment systems (Sun et al., 2019), impacts on the efficiency of wastewater treatment systems (Wang et al., 2022), and interference with the downstream water ecosystem (Sulistyowati et al., 2022). However, the mechanism by which the

* Corresponding author at: Key Laboratory of the Three Gorges Region's Eco-Environment, Ministry of Education, College of Environment and Ecology, Chongqing University, Campus B, 83 Shabeijie, Shapingba, Chongqing 400044, China.
** Corresponding author at: Key Laboratory of Coastal Environment and Resources of Zhejiang Province, School of Engineering, Westlake University, 18 Shilongshan Road, Hangzhou 310024, China.
E-mail addresses: chenyi8574@cqu.edu.cn (Y. Chen), Jufeng@westlake.edu.cn (F. Ju).

https://doi.org/10.1016/j.watres.2024.121506
Received 25 January 2024; Received in revised form 5 March 2024; Accepted 21 March 2024
Available online 22 March 2024

accumulation of plastic particles interferes with the nitrogen cycling and nitrous oxide (N_2O) release in water treatment systems is still unclear.

Constructed wetlands (CWs) are a green water-purifying system, in which biofilm system is the core unit of pollutant degradation (Wu et al., 2023). In the wetland biofilm system, the huge nitrification/denitrification potentials can remove most of ammonia and nitrate/nitrite and reduce the downstream eutrophication (Vymazal, 2007). Furthermore, CWs possess an excellent capacity to retain particle pollutants, thanks to the presence of abundant biofilms, and previous research indicated that over 90 % of metal(oxide) nanoparticles and micro/nano-sized plastics were captured in CWs (Ma et al., 2021; Yang et al., 2020). These trapped particle pollutants remain within CW system, preventing migration or outflow due to increased infiltration volume and concentration (O'Connor et al., 2019). Consequently, CWs serve as an effective barrier against plastic particles entering the aquatic environment.

Despite the prominent role of CWs as an important barrier of plastic particles to the natural aquatic ecosystem, recent studies have showed that plastic size-dependent effects in the CWs may affect nitrogen-removing process via altering microbial community structure and key enzyme activities with the long-term accumulation (Yang et al., 2020, 2022, 2022). However, whether and how the plastic size-dependent effects disturb N_2O production and release in nitrogen-removing processes of CWs are unclear at present. As we known, N_2O is a byproduct of nitrification and a medial-product of denitrification (Law et al., 2012), and the amount of N_2O released in the normal nitrogen removal process is up to $2.3 \times 10^2 - 7.9 \times 10^3$ mg N_2O/(kg N) in each type of CWs (Vymazal et al., 2006; Ouyang and Lee, 2020). Consequently, CWs are an important hot spot for N_2O emission, and controlling N_2O release in CWs is conducive to alleviating the global warming potential (GWP, the GWP_{100} of N_2O is about 265 times that of CO_2 for 100-year time horizons (IPCC, 2014)) and is of great significance for ecosystem stability. Furthermore, due to their large biofilm system, CWs can also trap up to 90 % of plastic particles (Ma et al., 2021; Yang et al., 2022). Regrettably, there have been few reports on how the retained plastic particles interfere with the function of biofilm system and how they affect the production and release of N_2O during nitrogen transformation process in CWs.

The traditional understanding of formation of microbial community in CWs reside in the attached phase biofilm (up to 80 %) on the surface of substrate (Penesyan et al., 2021). At present, the differences in microbial abundance, community structure, and metabolic processes in the biofilms have been analyzed, along with individual and community changes of microorganisms caused by substrate materials (Fu et al., 2020), seasons and climates (Liang et al., 2017), hydraulic conditions (Zeng et al., 2021), and aquatic plants (Zhao et al., 2015) in CWs. However, the effects of plastic particles on wetland biofilms have not been systematically studied. Although previous studies demonstrated that plastic particles changed the oxygen mass transfer capacity and microbial community structure in wetland systems (Yang et al., 2022, 2022), the impacts of plastic particles accumulation on the function of biofilm system in CWs have not been comprehensively explored, especially in nitrogen metabolisms, carbon metabolisms, and electron/energy transfer efficiency. In addition, the changes in the metabolic level of nitrogen transformation of core microorganisms, can also affect the N_2O release, and all need to be more fully known.

In order to address the knowledge gap, we designed and conducted experiments using 12 CW devices fed with simulated municipal wastewater over a year, during which the nitrogen removal efficiency and N_2O release under the accumulation of different sizes (50–100 nm, 50–100 μm, and 500–1000 μm) of plastic particles were investigated. Under the influence of plastic particles, we aimed to answer three key questions: (1) How do different nitrogen conversion processes contribute to N_2O production from CWs? (2) How does the functional status of biofilms respond? (3) To what extent do plastic particles with different sizes regulate the N_2O release processes and functional microorganisms? Answering these questions will improve the understanding of the accumulative effects of plastic particles on the biofilm system and GWP in the wetland wastewater-purifying systems.

2. Materials and methods

2.1. Preparation of micro(nano)plastics and synthetic wastewater

The raw macro- (500–1000 μm) and micro- (50–100 μm) sized polystyrene (PS) plastics were obtained by grinding and sieving the non-additive parental PS columns (Beisile, Tianjin, China). The nano-sized (50–100 nm) PS plastic particles were purchased with the suspension state (CAS: 9003-53-6, 5 % *w/v*) (Aladdin, Shanghai, China). The detailed preparation procedures of plastic particles were supplied in our previous studies (Yang et al., 2020, 2022). In order to simulate the actual plastic particles concentrations in wastewater (26.23–1189 μg/L) [3, 4], PS powder and suspension were dispersed and diluted to 100 μg/L in the synthetic wastewater. The compositions of synthetic wastewater were approximately 200 mg/L COD, 30 mg/L TN, and 20 mg/L NH_4^+-N according to simulating the wetland systems mainly used to treat the municipal wastewater and stormwater runoff. The initial pH of synthetic wastewater was adjusted to 7.0-7.1 by injecting 4 M NaOH or 4 M HCl solution. Details of the composition profile are provided in the Supporting Information (Text S1).

2.2. Experimental design and procedures

The saturated vertical flow wetland microcosms were rectangular shaped boxes constructed of treated toughened plastics with a length of 0.3 m, a width of 0.3 m and a depth of 0.5 m depth. The total of twelve wetland microcosms were filled with gravel (diameter: 8–10 mm), planted with the aquatic cattail (*Typha latifolia*), and were kept in an air-conditioned greenhouse (25 °C and 425 μmol m^{-2} s^{-1} light intensity). We conducted the sequencing batch experiment for 370 days [including 74 batches, hydraulic retention time (HRT) is 5 days] and divided the whole experiment period into three stages (S1: day 0–5, S2: day 175–180, S3: day 365–370) according to the change of nitrogen-removing performance. To ensure the accuracy of results, the water level at the beginning and at the end of each batch was recorded, which was taken into account the deviation caused by evaporation when calculating the effluent concentration. Artificial wastewater was fed into the reactor via the pipe and drained via a tap on the bottom, and the water level was attuned to be 5 cm below the gravel bed surface (Yang et al., 2022; China, S. E. P. A. o. 2002) and were supplied in Supporting Information.

2.3. Contribution assessment of N_2O release

The washed-off biofilm samples were transferred to 30 mL brown headspace bottles with 10 mL of synthetic wastewater containing the isotopes of ^{15}N and ^{18}O and placed in a 25 °C water-bathing shaker at 100rpm for 1 h. Each group needs to complete the small-scale isotope labeling experiment according to the following four incubation groups (Table S1). After incubation, headspace gas from each bottle were collected using a syringe and transferred into gas collection bags, while the liquid is filtered through a 0.22 μm filter membrane and placed into 5 mL centrifuge tubes. The isotopic content of all test products was determined using the isotope ratio mass spectrometer (MAT-253, Thermo Fisher Scientific, USA). The contributing value of each process in different pathway to N_2O was illustrated in Fig. 2D and calculated using the following formulas (Wrage et al., 2005):

$$N_2O_{NCD} = (c^{15}N_2O_{IN2} / c^{15}NO_3^-{}_{IN2}) \times c^{15}NO_3^-{}_{IN3} \quad (I)$$

$$N_2O_{AD} = c^{15}N_2O_{IN2} \quad (II)$$

$$N_2O_{ND} = (cN_2^{18}O_{IN4} \times cf - 2/3\ N_2O_{NCD}) \times 2 \quad (III)$$

$$N_2O_{HD} = c^{15}N_2O_{IN1} - N_2O_{AD} - N_2O_{NCD} - N_2O_{ND} \quad \text{(IV)}$$

Where:

I: Nitrification-coupled denitrification process (NCD);
II: Autotrophic denitrification process (AD);
III: Nitrifier denitrification process (ND);
IV: Heterotrophic denitrification process (HD);

cf: A conversion factor (3.7) to account for the application of $H_2^{18}O$ at 1 atom % excess ^{18}O while ^{15}N-labelled NH_4NO_3 was applied at 10 atom % excess ^{15}N.

2.4. Biofilm assays

2.4.1. LDH and ROS assays

A total of 10 g gravel sample was used to assess lactate dehydrogenase (LDH) release and reactive oxygen species (ROS) production, following our prior procedures (Yang et al., 2020). Briefly, 15 mL of PBS (pH = 6.8) was added to a conical flask containing 10 g of gravel, which was thoroughly shaken (150 rpm) for 5 min at 25 °C, the supernatant was used to determine the LDH release according to the instructions of the LDH kit (Nanjing Jiancheng Technology Co., Jiangsu, China). For ROS assay, the biofilm was separated from gravel or plastic particles, and then it was re-suspended in NaCl solution and incubated with 20 μmol/L H_2DCF-DA (Molecular Probes, Invitrogen) for 30 min. The mixed liquor was transferred into 96-well microtiter plates for fluorescence spectroscopy at excitation/emission wavelengths of 495/525 nm.

2.4.2. Electron transport system activity, NADH and ATP assays

Approximately 10 g gravels were also sampled to measure electron transport system activity (ETSA) by reducing 2-(p-iodophenyl)-3-(pnitrophenyl)-5-phenyl tetrazolium chloride (INTC) to formazan according to a previous protocol with minor modifications (Su et al., 2019). Absorbance of the orange-like formazan was immediately detected at 490 nm against a solvent blank. After the long-term exposure experiment, NADH was detected using the enzymatic cycling assay (San et al., 2002). In brief, 10 g of the gravel samples were put into 50 mL conical flasks and washed thrice with 100 mM PBS (pH = 7.8). Then, 10 mL of 0.2 M NaOH were added to the conical flasks, and the flasks were placed in a water bath at 50 °C for 10 min and in ice water to cool to 4 °C. The samples were neutralized by adding 0.2 M HCl, and after centrifugation at 16,000 rpm for 5 min, the supernatants were immediately collected to measure the NADH content (details about the process are presented in our previous study (Yang et al., 2020)). The ATP level was measured using the ATP Assay Kit (Nanjing Jiancheng Biological Engineering, China), according to the manufacturer's instructions.

2.4.3. Nitrification and denitrification rates

Nitrification and denitrification rates were assessed according to our previous study (Yang et al., 2022). Briefly, nitrification rate was expressed using the slope of the first-order function of total NO_2^--N and NO_3^--N concentrations in solution and time. Denitrification rate was detected using isotope labeling technology and were calculated by $^{29}N_2$ and $^{30}N_2$ content in the gaseous product (^{15}N pairing technique).

2.4.4. DNA extraction, library construction, and metagenomic sequencing

Extraction of DNA from each biofilm sample was performed using FastDNA SPIN Kit for Soil (MP Biomedicals, Solon, OH, USA) according to the manufacturer's instructions. DNA extract was fragmented to an average size of about 300 bp using Covaris M220 (Covers, USA) for paired-end library construction. Paired-end library was constructed using NEB Next® Ultra™ DNA Library Prep Kit for Illumina (NEB, USA). Paired-end sequencing was performed on Illumina Hiseq™ 2500 platform (Illumina, USA) using TurSeq PE Cluster Kit according to the manufacturer's instructions. The bioinformatic procedures are described with more details in our previous study (Yang et al., 2022). The sequence data were deposited into CNGB Sequence Archive (CNSA) China National GeneBank DataBase (CNGBdb) (Chen et al., 2020) with accession number CNP0001921.

2.5. Microbial metabolism analysis

2.5.1. Enzyme activity assay

Key enzyme activities involved in microbial metabolism and denitrification process can reflect the pollutant-induced potential effects. At the end of each stage during exposure experiment, approximately 250 g of gravels were collected from three depths (10, 25, and 40 cm) and subjected to tests for ammonia monooxygenase (AMO), Hydroxylamine oxidoreductase (HAO), nitrate reductase (NAR), nitrite reductase (NIR), nitric reductase (NOR), nitrous oxide reductase (NOS), ribulose 1,5-bisphosphate carboxylase (RubisCO), hexokinase (HK), glyceraldehyde-3-phosphate dehydrogenase (GAPDH), pyruvate kinase (PK), phosphofructose kinase (PFK). The details of these procedures were conducted as in our previous studies (Su et al., 2019; Yang et al., 2018). The final value was the average value of samples collected at three depths.

2.5.2. Metagenomic analysis

The raw data of metagenomic sequencing was checked for quality and treated using FastQC (version 0.11.7) (Andrews, 2010) and Fastp (version 0.19.7) (Chen et al., 2018), respectively, to get the clean reads. Because a specialized reference database of functional genes coding the key proteins involving the biofilm-forming proteins, N-ion transporters, and key C metabolic enzymes is limiting, a core gene (CGs) dataset was self-created. The description and sequence constituent of each core gene was summarized in Dataset 1. To enable fast and accurate quantification of biofilm-forming protein and N-ion transporter genes in metagenomic data, a two-step successive annotation strategy was deployed to quantify reads. This strategy successively aligns each metagenomic read against the customized CGs database using DIAMOND (Buchfink et al., 2021). For N metabolic gene annotation, the clean reads of shotgun metagenomes were searched against NCyc database (Tu et al., 2019). Then, the best-hit reads assigned to each gene were counted and used for further calculation of normalized relative abundance (see the next section for details).

To predict the microbial hosts of functional genes (Dataset 1) involved in microbial N cycle, carbon metabolism, and biofilm formation, the metagenomic reads assigned to the functional genes in NCyc and CGs database were extracted and then subjected to the taxonomic assignment using Kraken 2 (Wood et al., 2019). The taxonomic profiles for each functional gene involved in microbial N cycle and biofilm-formation were generated by calculating the relative abundance of each assigned taxon (Dataset 2).

The relative abundance (*RA*) of genes we focused in our analysis was computed as the reads per kilobase (RPK) of the gene divided by the sum of RPK of all sequenced 16S rRNA gene pre-determined by ARG-OAP database (Rognes et al., 2016) with the alignment identity cutoff of 0.9, referenced to the general taxonomic thresholds to distinct phyla (Yarza et al., 2014), against the 16S rRNA gene sequence dataset of SILVA SSU Ref 138.1 with 90 % identity criterion (Quast et al., 2013). The following equation that deploys the above calculation method for the 16S-normalized relative abundance (gene copy/16S rRNA gene copy, GP16S) of a gene in a metagenome (Ju et al., 2019) were expressed as follows:

$$RPK = \frac{\sum_1^n N_{nucleobase\ mapped} \Big/ L_{read\ length}}{L_{gene\ length} \Big/ 1000} \quad \text{(V)}$$

$$RA = \mathrm{RPK(Gene)} \Big/ \sum_1^n RPK(16S) \quad \text{(VI)}$$

Where:

$\sum_1^n N_{nucleobase\ mapped}$: The number of all nucleobases mapped to the gene;
$L_{\ read\ length}$: The length of the read;
$L_{\ gene\ length}$: The length of the gene;

RPK (16S): RPK of 16S rRNA gene reference sequence.

2.6. Statistical analysis

The assays of all experiments were conducted in triplicate, and the results were presented as the mean ± standard deviation. Analysis of variance (ANOVA) was used to compare results by group. All description of significant differences in this paper were conducted the statistically significant test (meaning $P < 0.05$, SPSS 22.0, IBM).

3. Results

3.1. Plastic particles affecting the CW performance

3.1.1. Change in N-removing performance

In a 370-day nitrogen-removing efficiency test on CWs, three stages (early, middle, and late) were observed based on the trend of treatment performance. As shown in Fig. 1, introducing plastic particles of different sizes resulted in stable outflow NH_4^+-N concentrations of 2.89 ± 0.75 mg/L (86.5 ± 0.04 % removal rate) and no $NO_{3(2)}^-$-N accumulation during the first stage (Fig. 1A). At the middle stage, NH_4^+-N concentrations varied across groups, with only the Nano group showing $NO_{3(2)}^-$-N accumulation (Fig. 1B). In the late stage, NH_4^+-N concentrations significantly increased in the Nano and Micro groups, along with $NO_{3(2)}^-$-N accumulation in Nano group (Fig. 1C). Overall, long-term accumulation of plastic particles in CWs had different degrees of impacted NH_4^+-N removal (Micro- < Micro- < Nano-sized plastics), but the only nano-sized particles were found to hinder $NO_{3(2)}^-$-N reduction. Intriguingly, large-sized particles even exhibited a promoting effect on $NO_{3(2)}^-$-N removal during the whole experiment.

3.1.2. Change in N_2O emission

As shown in Fig. 2A–C, N_2O release in the early-stage of the three treatment groups did not differ from the control group except that the N_2O concentration fluctuated during a batch for the Macro group. Yet, in later stages, a size-dependent trend emerged, with suppression observed in the Nano group. Furthermore, we found that the long-term accumulation of plastic particles changed the contribution pattern of N_2O in different nitrogen-removing processes in CWs (Fig. 2D and E). Detailly, during nitrification-coupled denitrification, large size groups showed reduced N_2O release contribution, with the Macro group leading (61.3 % reduction, Table S2). In the hydroxylamine reduction process, though the release contribution of N_2O as the byproduct in ammoxidation in all groups had no difference, the release capacity significantly decreased in all groups, with the Nano group leading (66.2 % reduction), followed by Macro (55.6 %) and Micro (41.1 %) (Table S2). For nitrifier denitrification, the release contribution of N_2O in all groups had significantly increase, meanwhile Micro and Nano groups increased N_2O release by 77.2 % and 39.9 % (Table S2), respectively. For denitrification, the release contribution of N_2O showed a decrease trend in large size groups, while all groups saw significant N_2O release reductions (ranging from 47.0 % to 65.2 %, Table S2).

3.2. Responses of biofilm function to plastic particles

In our study, we assessed biofilm responses to plastic particle accumulation by measuring reactive oxygen species (ROS) and lactate dehydrogenase (LDH) release. Fig. S1A shows that ROS decreased with plastic accumulation in the Macro and Micro groups but rose significantly in the Nano grou, which also displayed the highest LDH release, indicating microbial membrane damage due to ROS (Cordeiro, 2014). We also quantified electronic transfer efficiency (ETE) activity, energy (ATP) and electron (NADH) carrier levels within the biofilm (Fig. S1B), and larger plastic particles enhanced these indicators, while nano-sized plastic accumulation significantly inhibited ETE activity (by 77.8 %), along with ATP (by 74.5 %) and NADH (by 83.7 %) content, compared to the control group. These changes impacted N-removing bacterial activity and N-removing efficiency. For instance, the Nano group's denitrification rate was only 79.8 % of the control, and all plastic particle sizes hindered the nitrification rate by 52.1 % (Macro group) to 21.7 % (Nano group) (Fig. S1C), thus possibly explaining the reduced N_2O release in the treatment groups.

3.3. Chronic effects of plastic particles on microbial metabolism

3.3.1. Nitrogen ion transmembrane transport

Our study investigated the impact of plastic particle accumulation on microbial N-ion transmembrane transport in CWs through gene abundance analysis. In Fig. 3A, ATP-binding protein-coding genes *nrt*D and *cyn*D, part of the nitrate/nitrite transport system, declined in all treatment groups, with the most significant drop in the Nano groups. Conversely, *nrt*C and *nas*D increased in the Macro and Micro groups but decreased only in the Nano group (Fig. 3B). Genes encoding osmotic enzyme proteins (*nrt*B, *nas*E, and *cyn*B) remained consistent with the change of *nrt*C and *nas*D among treatments (Fig. 3C). However, genes *nrt*A, *nas*F, and *cyn*A decreased by 66.1 % in the Nano group (Fig. 3D). The key ammonium transporter gene (*amt*) also declined in all groups,

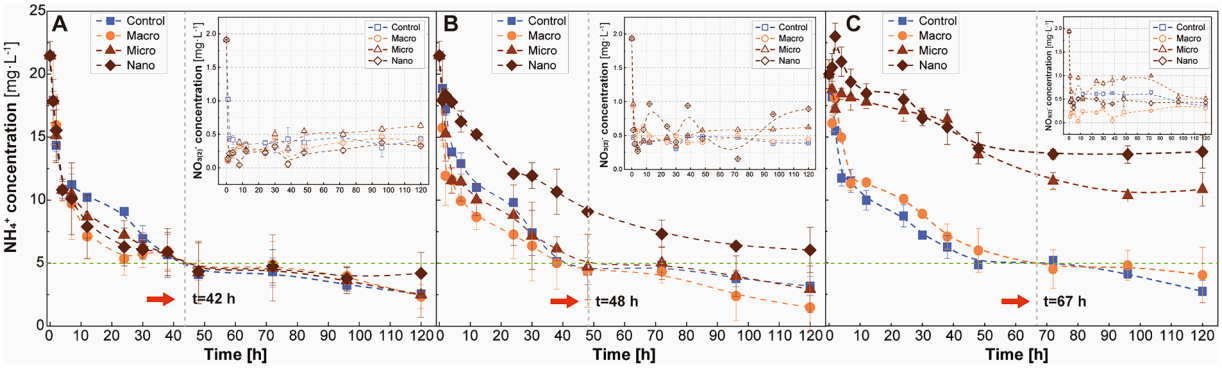

Fig. 1. Variations of NH_4^+-N and $NO_{3(2)}^-$-N concentrations during three typical batches at the start of experiment. Based on the change of nitrogen-removing performance of constructed wetlands (CWs) exposing to different concentrations of MNPs, the whole experiment period was divided into three stages: A, Early-stage, day 0–5; B, Middle-stage, day 175–180; C, Last-stage, day 365–370. The green-broken line is the GB18918-2002 1A discharge standard in China, and the grey-broken lines are the time to achieve the 1A.

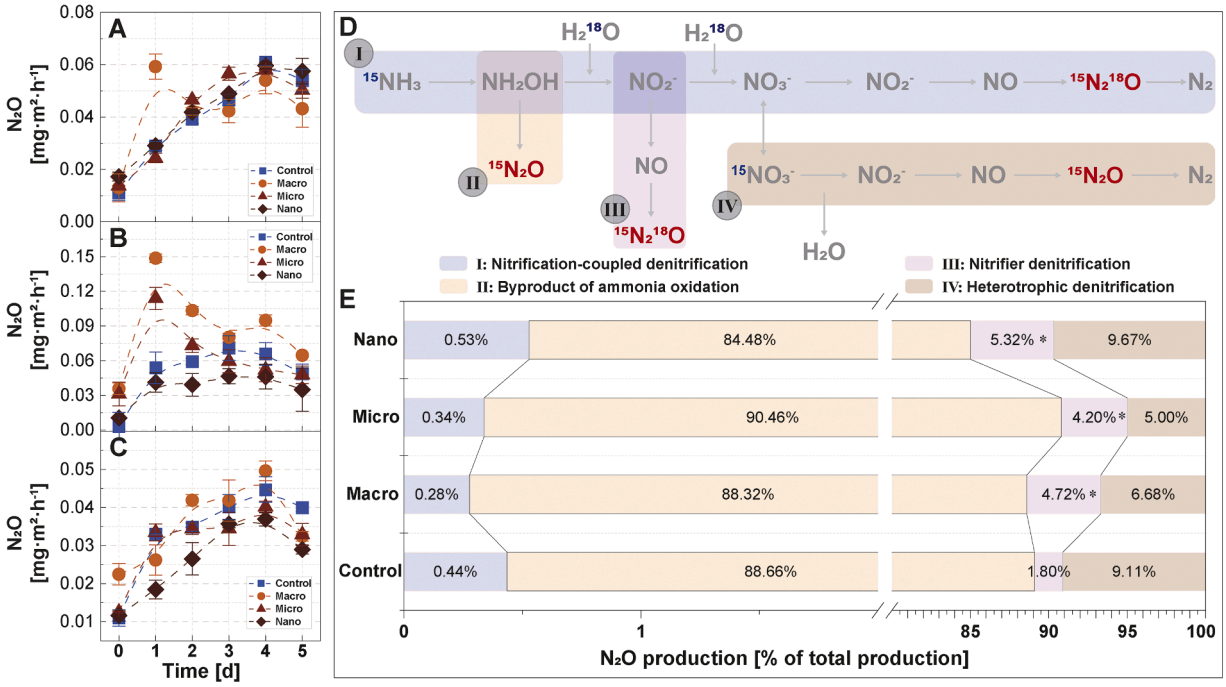

Fig. 2. N_2O fluxes of the constructed wetlands (CWs) under feeding of plastics with different sizes from macro to micro and nano-scales. A–C, N_2O release from the CWs at the Early-stage (A), Middle-stage (B) and Last-stage (C). D-E, relative contributions of denitrification, nitrification, nitrification-coupled denitrification, heterotrophic denitrification to $^{15}N_2O$ production in wetland systems exposing to different sizes and concentrations plastic particles for 370 days. Data are presented as the means ± standard deviation of triplicate tests, and asterisks (*) indicate significant differences from the control group ($P < 0.05$).

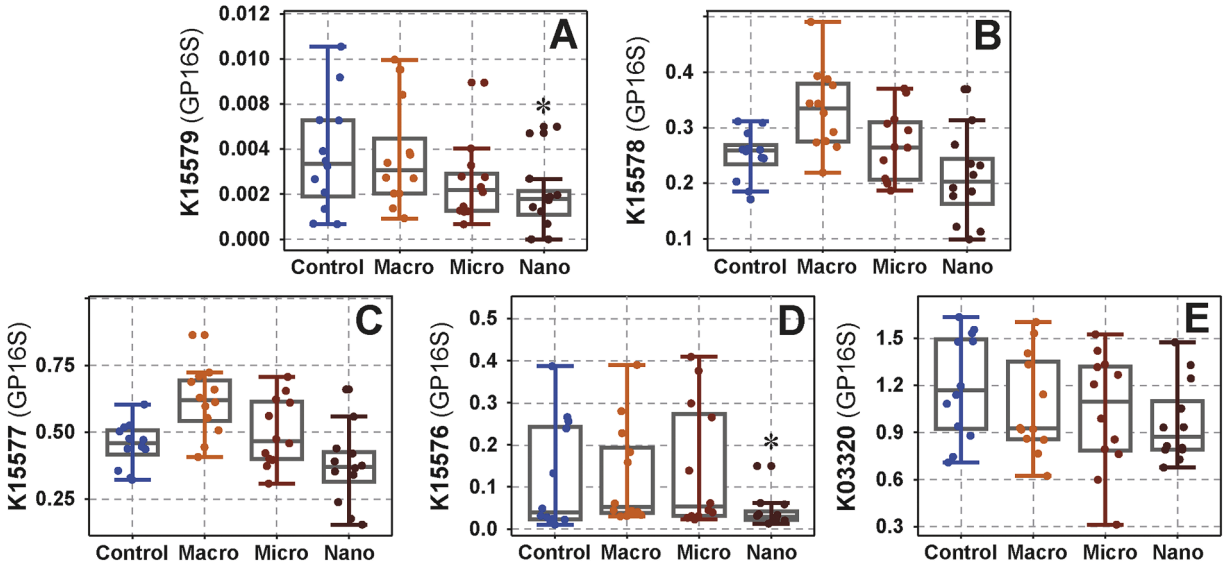

Fig. 3. Changes of the key gene abundance involving in the transmembrane transport of nitrogen ions between the intra- and extra-cellular region under exposing to the 370-day accumulation of plastic particles in CWs (A: *nrt*D and *cyn*D encoding to the nitrate/nitrite transport system ATP-binding protein, B: *nrt*C and *nas*D encoding to the nitrate/nitrite transport system ATP-binding protein. C: *nrt*B, *nas*E, and *cyn*B encoding to the nitrate/nitrite transport system permease protein, D: *nrt*A, *nas*F, and *cyn*A genes encoding to the nitrate/nitrite transport system substrate-binding protein, and E: *amt* gene encoding to ammonium transporter). Asterisks (*) indicate significant differences from the control group ($P < 0.05$).

especially in the Nano group (Fig. 3E). Prolonged plastic particle exposure negatively affected microbial nitrogen ion absorption capacity in CWs, with the most significant impact from Nano-sized particle.

3.3.2. *Nitrogen metabolism*

Key genes for ammonia oxidation (*amo*A/B/C) were more abundant in the Micro groups but significantly lower in the Nano group. Both Macro and Micro groups showed increased AMO activity, while the Nano group exhibited a 40 % decrease (Fig. 4A). Concerning key gene *hao* and enzyme HAO in hydroxylamine oxidation, all groups down-regulated *hao* abundance, while the Micro group exhibited a significant decrease, and HAO activity was significantly inhibited in all treatment groups (Fig. 4B). In the denitrification process, nitrate reductase genes (*nar*G/H/I) decreased in abundance in all groups, with NAR activity increasing in the Macro group but decreasing in the Micro and Nano groups (Fig. 4C). Nitrite reductase NIR gene abundance increased in all

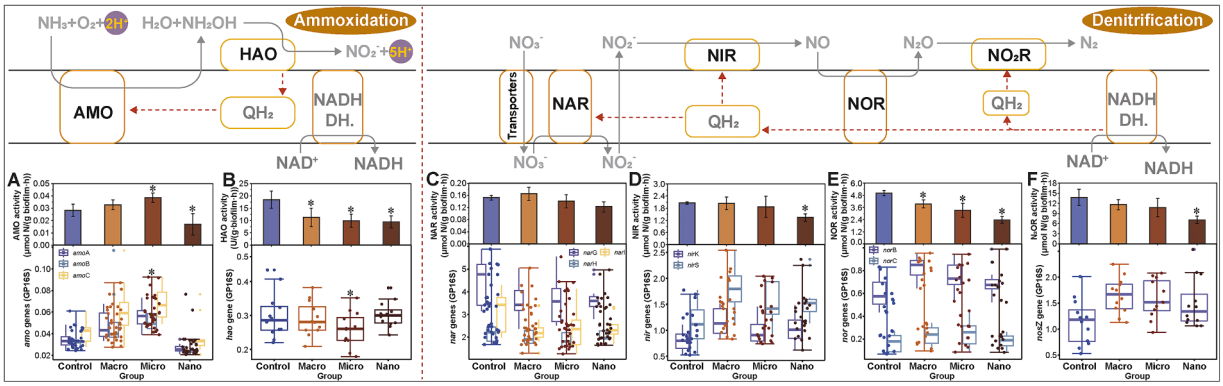

Fig. 4. Responses of key enzyme activity and the corresponding gene abundance involving in nitrogen-transforming process to the 370-day accumulation of plastic particles in CWs. A: ammoxidation, B: hydroxylamine oxidation. C: Nitrate reduction, D: Nitrite reduction, E: Nitric oxide reduction, and F: Nitrous oxide reduction. Asterisks (*) indicate significant differences from the control group ($P < 0.05$) based on ANOVA tests.

groups, but NIR activity decreased in the Nano group by 35 % (Fig. 4D). Nitric oxide reductase NOR gene abundance increased, while NOR activity significantly decreased in all treatment groups (Fig. 4E). In the final denitrification stage, *nos*Z gene abundance increased in all groups, but N_2OR activity was notably inhibited, especially in the Nano group with a 48.3 % decrease (Fig. 4F).

3.3.3. Carbon metabolism

Carbon metabolism is essential for microbial physiological activities, including energy (ATP) and electron (NADH) production. In Fig. S2, the average abundance of *rbc*L/S genes encoding the RubisCO enzyme decreased in the treatment groups, and RubisCO enzyme activity significantly dropped by 43.6 % in the Macro group and by 66.9 % in the Nano group (Fig. S2A). The *gap* gene, which produces NADH during glycolysis, decreased in the Macro, Micro, and Nano groups, and GAPDH enzyme activity also notably decreased by 67.3 % and 58.2 % (Fig. S2B). The gene *hk*, responsible for converting glucose to small carbon sources during glycolysis, also declined in the Macro, Micro, and Nano groups (Fig. S2C). The genes encoding PFK (*pfk*) and PK (*pk*) enzymes, involved in ATP production during glycolysis, increased in all three treatment groups (Fig. S2D). Although no significant difference appeared in *pk* gene abundance, the activities of PFK and PK enzymes decreased by 39.2 % and 61.5 % in the Nano group (Fig. S2E). PDH enzyme, a critical link between glycolysis and the citric acid cycle, significantly affects microbial energy and electron generation. The abundance of *pdh*A/B and *ace*E genes showed no significant differences among the groups, while PDH enzyme activity significantly dropped by 51.3 % in the Nano group (Fig. S2F).

3.4. Plastic particles altering the main species composition

Fig. S3 illustrates how long-term plastic particle accumulation may impact nitrogen cycling in CWs by reshaping the community structure of core species with key functional genes. Core species encoding genes involved in nitrogen metabolism, such as *amo*A/B/C, *hao*, and *pmo*, were mainly *Nitrosomonas* across all groups. However, their proportion was lowest in the Nano group and significantly varied. Core species related to *amo*A/B/C genes, like *Nitrosospira* and *Nitrosomonadaceae* for *hao*, and *Methylocystis* for *pmo*, exhibited substantial abundance changes, particularly in the Nano group. In the nitrification process, core host species for the key enzyme nitrite oxidoreductase (NXR) included *Nitrobacter* and *Nitrospira*, with decreased abundance in all treatment groups, most notably in the Nano group, where *Nitrospira* was affected the most. The nitrate reduction process saw variations in core species involved in assimilatory and dissimilatory pathways. *Thauera, Streptomyces, Pseudomonas*, and *Proteobacteria* were core hosts for genes *nar*B and *nas*A/B. Their abundance was higher in the Macro and Micro groups but significantly lower in the Nano group, particularly *Thauera* and *Pseudomonas*. Similarly, *Actinobacteria, Streptomyces, Tessaracoccus*, and *Pseudomonas* were main hosts for both *nir*B/*nrf*A and *nir*A genes, while Arthrobacter, *Micromonospora, Mycobacteriaceae, Nitrospira, Azoarcus, Burkholderiales, Microbacterium*, and *Thauera* were main hosts with either assimilatory or dissimilatory nitrite reduction genes, showing higher abundance in the Macro and Micro groups but significantly lower in the Nano group. During denitrification, key genes such as *nir*K/S, *nor*B/C, and *nos*Z were primarily hosted by *Proteobacteria, Pseudomonas, Azoarcus, Anaeromyxobacter, Azoarcus, Dechloromonas*, and *Thauera*. These denitrifiers increased significantly in the Macro and Micro groups, especially *Dechloromonas, Pseudomonas*, and *Thauera*, while most denitrifiers decreased in abundance in the Nano group. The *nif*H gene, encoding the nitrogenase, was mainly hosted by *Desulfovibrio, Dechloromonas*, and *Geobacter*, with different abundances among groups. In conclusion, long-term plastic particle accumulation led to significant changes in the core species composition and function in the nitrogen cycling process of CWs, potentially affecting nitrogen removal efficiency and N_2O release.

4. Discussion

Our previous research demonstrated that, compared to plastic concentration, the size of plastic particles has a more pronounced impact on the self-assembly of microbial communities and denitrification efficiency in CWs during the accumulation process (Yang et al., 2022). However, the mechanisms underlying the effect differences of varying sized plastics on microbial N_2O release in nitrogen-removing processes, have not been addressed. This study building upon our previous research provides a detailed exploration and analysis of these mechanisms, where we concluded the three mechanism pathways of N_2O release reduction as depicted in Fig. 5. Pathway A: Macro-sized plastics, serving as carriers for biofilms (Fig. 5A), diminish the activity of autotrophic microbial CO_2 assimilation, which weaken the metabolic capacity of ammoxidation, as well as finally reduced the release of N_2O as a byproduct (path II in Fig. 2D); Pathway B: Microbes adhere to micro-sized plastics without forming biofilms (Fig. 5B), decreasing *amo* genes abundance and HAO activity in ammoxidation process and consequently lowering nitrification capacity and reduced the production of N_2O (path III in Fig. 2D); Pathway C: Nano-sized plastics can adhere to microbial surfaces and penetrate cell membranes (Fig. 5C), affecting periplasmic N-ion transmembrane and reductase activities (Fig. 3), which ultimately impacts the N_2O production and release in nitrification and denitrification processes (all of paths in Fig. 2D).

Our study has the same conclusion as He et al. (2022), and further refined the microbial pathway of mitigation and the possible metabolic change mechanism. Meanwhile, our findings also challenge the previous

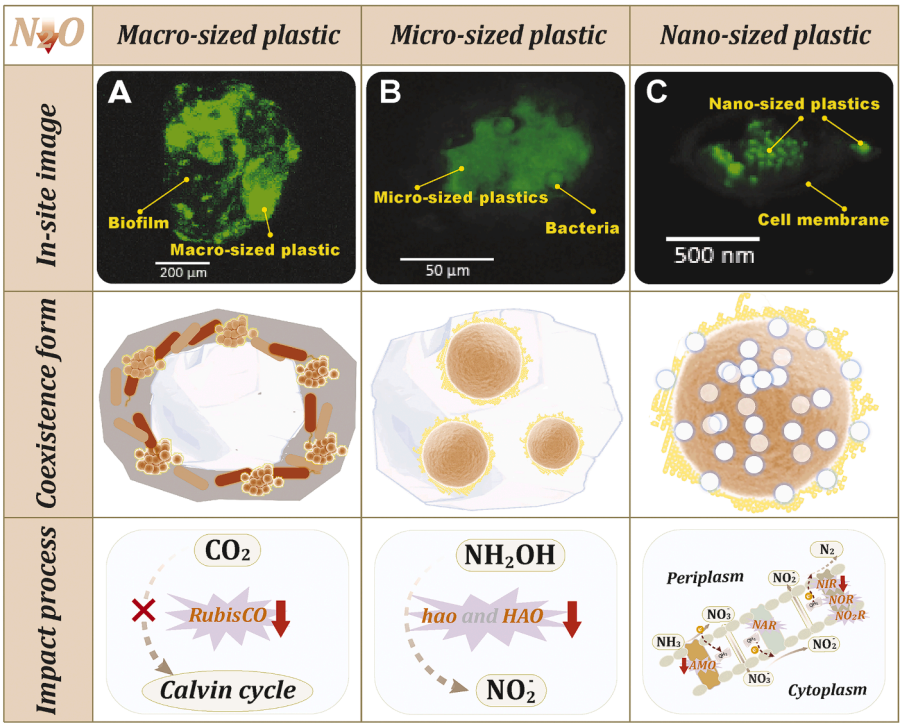

Fig. 5. Mechanisms schematic diagram involving in the reduction of N_2O emissions in CWs caused by different-sized plastic particles. Pathway A: macro-sized plastics form attached biofilms, weakening inorganic carbon (i.e., CO_2) assimilation in the nitrification process, which, in turn, reduces carbon energy metabolism, ultimately lowering N_2O emissions. Pathway B: Bacteria extensively adhere to micro-sized plastics, reducing key gene abundance in ammonia oxidation and subsequently lowering nitrous oxide emissions as a byproduct of nitrification. Pathway C: Nano-sized plastics accumulate on microbial membrane and intercellular region, influencing N-ion transmembrane and reductase activities, which diminished N_2O release in nitrogen cycle.

notions of severely promoting effects from microplastics or nanoplastics on N_2O release in environmental medium (Yu et al., 2021; Chen et al., 2022). Previous studies often followed *in-situ* sampling and laboratory-scale experiments when observing the introduction of plastic particles or biodegradable plastics (Nelson et al., 2022; Seeley et al., 2020). Not only that, previous researches focused solely on denitrification processes and ignored microbial interactions with microplastics and varied nitrogen metabolism contribution in realistic environmental conditions (Su et al., 2022; Zhou et al., 2023). Hence, these might result in conflicting conclusions regarding the effect of microplastic accumulation on N_2O release. Additionally, the fungal denitrification typically results in N_2O as a final product, while in CWs the fungal denitrification is relatively weak and not sufficient to impact overall N_2O release, which explain the differences with the research of estuarine sediment reported by Su et al. (2022). Subsurface flow wetlands, with abundant liquid water and free-living microbes alongside biofilms, enhance microbial organic matter utilization and denitrification efficiency. Furthermore, larger plastic particles typically have negatively charged surfaces and can effectively adsorb positively charged ions like copper and iron (Prata et al., 2019) as essential core elements of key enzymatic sites in nitrogen-removing microbes (AMO, NAR, and NIR) (Zumft, 1997), as well as crucial components of cytochromes and quinone pool proteins being responsible for the electron transfer (Simon et al., 2000), which enhanced electron transfer efficiency and microbial activity in large-size treated CWs. All of these processes can enhance N_2O conversion to N_2 during denitrification, as well as assisting to reduce the byproduct N_2O of nitrification, which also explains the decrease in the ratio of N_2O release in heterotrophic denitrification and N_2O reduction in Macro and Micro groups.

Importantly, in order to prove the weaken of NH_2OH transforming to N_2O in nitrification caused by the decreased assimilation ability of inorganic carbon in large-sized groups, we, for the first time, focused on the carbon metabolism process of ammonia-oxidizing microorganisms assimilating inorganic carbon. The results revealed a significant reduction in the activity of the carbon-fixing enzyme RubisCO in all groups, leading to organic carbon source blockade for chemolithoautotrophic nitrifiers and a marked decrease in ammoxidation activity. Eminently, nano-sized plastics significantly inhibited almost all of key enzyme activities in the Calvin cycle, glycolysis, and tricarboxylic acid cycle processes (Fig. S2), which also explains the direct link between reduced nitrogen transformation efficiency and carbon metabolism blockage. Previous research on microbial stress caused by particle pollutants has explained that those possess unique physicochemical properties, including a large specific surface area, which can adsorb various ions and organic substances, exerting toxicity on microorganisms (Liu et al., 2023). Especially, nanomaterials often feature superoxide radical groups with oxidative and antibacterial effects. Similarly, nano-sized plastics produce similar functional groups under light or aging conditions (Du et al., 2023), further diminishing microbial activity. Moreover, nano-sized plastics raise the concentration of reactive oxygen species in microorganisms, indirectly disrupting microbial metabolic processes (N and C metabolisms) (Yang et al., 2020). Nano-sized plastics adhering to microbial cell membranes not only reduce microbial metabolic activity but also interfere with cell membrane formation and function (i.e., N-ions transmembrane transport) (Tan et al., 2020; Zhu et al., 2022).

This study provides a mechanistic understanding on how varying sized plastic particles influence N_2O release in CWs via mediation on the various nitrogen transformation processes. It uncovers the response mechanisms in CWs to the long-term accumulation of plastic particles, considering macroscopic changes in biological processes and microscopic alterations in key enzyme activity and functional gene abundance in microbial N and C metabolisms. The findings reveal that plastic particles inhibited the hydroxylamine reductase activity and CO_2 assimilatory capacity in the ammoxidation process reducing nitrogen removal efficiency and N_2O release. Differently, nano-sized plastics disrupt crucial microbial metabolic processes, leading to the decrease in

N-ion and electron transfer capacity and N-reductase activities. In summary, over the long-term accumulation, all sized plastics in CWs ultimately will weaken N_2O release with the different influencing mechanisms, and importantly it was with the extent of influence inversely related to particle sizes. Our study can be basis to inspire this innovative work on the mechanisms for affecting N_2O release.

Overall, in this study, we utilized ^{15}N and ^{18}O isotope tracing to discern alterations in pathways contributing to N_2O release in CWs under plastic particle interventions. Through microbial analysis, we identified the factors underlying differences in N_2O release contributions. Starting from the surface-level detection of N_2O release to an exploration of inherent microbial metabolic mechanisms, our findings revealed that plastic particles of varying sizes decreased N_2O production and release in CWs through diverse influencing pathways. The degree of intervention is inversely proportional to particle size. Simultaneously, our conclusion provides pivotal information challenging the prevailing negative stereotype of plastic particles in ecosystems.

Plastic particle, as emerging environmental pollutant, has garnered extensive attention and research interest. Without exception, reports on plastic particle have been predominantly negative, citing concerns such as deformities in aquatic animals, the dissemination of additional pollutants, and decreased efficiency in water treatment systems. These unfavorable reports have ingrained a stereotypical perception that microplastics can only exert adverse effects on the environment, disrupting ecosystem stability. However, our study offers a counterintuitive conclusion. The accumulation of plastic particle in wetland systems intervenes in the metabolism of nitrogen-cycling microorganisms, ultimately reducing N_2O production and release. Globally, diverse wetland systems stand as significant sources of N_2O. The current global environmental emphasis lies in regulating nitrogen cycling in wetland systems to curtail N_2O release, a crucial pathway toward achieving the global "double carbon" goals. Drawing upon our study's findings, we posit that particles of equivalent size in wetland systems may trigger analogous intervention mechanisms. Strategically employing inorganic particles that pose no harm to ecological wetland systems to mitigate N_2O release could potentially yield substantial environmental benefits. This, fundamentally, constitutes the overarching environmental significance of our study.

CRediT authorship contribution statement

Xiangyu Yang: Writing – original draft, Visualization, Formal analysis, Data curation, Conceptualization. **Yi Chen:** Writing – review & editing, Writing – original draft, Supervision, Methodology, Conceptualization. **Tao Liu:** Investigation, Data curation. **Lu Zhang:** Visualization, Formal analysis. **Hui Wang:** Visualization, Formal analysis. **Mengli Chen:** Investigation, Data curation. **Qiang He:** Writing – review & editing, Funding acquisition. **Gang Liu:** Writing – review & editing. **Feng Ju:** Writing – review & editing, Supervision, Formal analysis.

Declaration of competing interest

The authors declare that they have no known competing financial interests or personal relationships that could have appeared to influence the work reported in this paper.

Data availability

Data will be made available on request.

Acknowledgments

This work was supported by the "National Natural Science Foundation of China (51978099 and 52200077)" and "Program of Distinguished Young Scholars, Natural Science Foundation of Chongqing, China (CSTB2022NSCQ-JQX0023)".

Supplementary materials

Supplementary material associated with this article can be found, in the online version, at doi:10.1016/j.watres.2024.121506.

References

Andrews, S.O., 2010. FastQC: a quality control tool for high throughput sequence data.
Buchfink, B., Reuter, K., Drost, H.G., 2021. Sensitive protein alignments at tree-of-life scale using DIAMOND. Nat. Methods 18 (4), 366. -+.
Chen, S., Zhou, Y., Chen, Y., Gu, J., 2018-i890. fastp: an ultra-fast all-in-one FASTQ preprocessor. Bioinformatics 34 (17), i884.
Chen, F.Z., You, L.J., Yang, F., Wang, L.N., Guo, X.Q., Gao, F., Hua, C., Tan, C., Fang, L., Shan, R.Q., Zeng, W.J., Wang, B., Wang, R., Xu, X., Wei, X.F., 2020. CNGBdb: China National GeneBank DataBase. Yi Chuan 42 (8), 799–809.
Chen, C., Pan, J., Xiao, S., Wang, J., Gong, X., Yin, G., Hou, L., Liu, M., Zheng, Y., 2022. Microplastics alter nitrous oxide production and pathways through affecting microbiome in estuarine sediments. Water Res. 221, 118733.
China, S. E. P. A. o., 2002. Standard Methods for the Examination of Water and Wastewater (4th version). Environmental Science Publication in China, Beijing.
Cordeiro, R.M., 2014. Reactive oxygen species at phospholipid bilayers: distribution, mobility and permeation. Biochim. Biophys. Acta Biomembr. 1838 (1), 438–444.
Du, T., Yu, X., Shao, S., Li, T., Xu, S., Wu, L., 2023. Aging of nanoplastics significantly affects protein corona composition thus enhancing macrophage uptake. Environ. Sci. Technol. 57 (8), 3206–3217.
Fu, G., Wu, J., Han, J., Zhao, L., Chan, G., Leong, K., 2020. Effects of substrate type on denitrification efficiency and microbial community structure in constructed wetlands. Bioresour. Technol. 307, 123222.
He, Y., Liu, Y., Yan, M., Zhao, T., Liu, Y., Zhu, T., Ni, B.J., 2022. Insights into N_2O turnovers under polyethylene terephthalate microplastics stress in mainstream biological nitrogen removal process. Water Res. 224, 119037.
IPCC, 2014. Climate Change 2014: Synthesis Report. Contribution of Working Groups I, II and III to the Fifth Assessment Report of the Intergovernmental Panel no Climate Change [Core Writing Team. IPCC, Geneva, Switzerland, p. 151.
Ivleva, N.P., 2021. Chemical analysis of microplastics and nanoplastics: challenges, advanced methods, and perspectives. Chem. Rev. 121 (19), 11886–11936.
Ju, F., Beck, K., Yin, X.L., Maccagnan, A., McArdell, C.S., Singer, H.P., Johnson, D.R., Zhang, T., Bürgmann, H., 2019. Wastewater treatment plant resistomes are shaped by bacterial composition, genetic exchange, and upregulated expression in the effluent microbiomes. ISME J. 13 (2), 346–360.
Koelmans, A.A., Redondo-Hasselerharm, P.E., Nor, N.H.M., de Ruijter, V.N., Mintenig, S. M., Kooi, M., 2022. Risk assessment of microplastic particles. Nat. Rev. Mater. 7 (2), 138–152.
Law, Y., Ye, L., Pan, Y., Yuan, Z., 2012. Nitrous oxide emissions from wastewater treatment processes. Philos. Trans. R. Soc. B Biol. Sci. 367 (1593), 1265–1277.
Liang, K., Dai, Y., Wang, F., Liang, W., 2017. Seasonal variation of microbial community for the treatment of tail water in constructed wetland. Water Sci. Technol. 75 (10), 2434–2442.
Liu, T., Guo, F.C., Chen, M.L., Zhao, S.Y., Yang, X.Y., He, Q., 2023. Silver nanoparticles disturb treatment performance in constructed wetlands: Responses of biofilm and hydrophyte. J. Clean. Prod. 385, 135751.
Ma, Y., Huang, J., Han, T., Yan, C., Cao, C., Cao, M., 2021. Comprehensive metagenomic and enzyme activity analysis reveals the negatively influential and potentially toxic mechanism of polystyrene nanoparticles on nitrogen transformation in constructed wetlands. Water Res. 202, 117420.
MacLeo, M., Arp, H.P.H., Tekman, M.B., Jahnke, A., 2021. The global threat from plastic pollution. Science 373 (6550), 61–65 (1979).
Nelson, T.F., Baumgartner, R., Jaggi, M., Bernasconi, S.M., Battagliarin, G., Sinkel, C., Kuenkel, A., Kohler, H.P.E., McNeill, K., Sander, M., 2022. Biodegradation of poly (butylene succinate) in soil laboratory incubations assessed by stable carbon isotope labelling. Nat. Commun. 13 (1), 5691.
O'Connor, D., Pan, S., Shen, Z., Song, Y., Jin, Y., Wu, W.M., Hou, D., 2019. Microplastics undergo accelerated vertical migration in sand soil due to small size and wet-dry cycles. Environ. Pollut. 249, 527–534.
Ouyang, X., Lee, S.Y., 2020. Improved estimates on global carbon stock and carbon pools in tidal wetlands. Nat. Commun. 11 (1), 317.
Penesyan, A., Paulsen, I.T., Kjelleberg, S., Gillings, M.R., 2021. Three faces of biofilms: a microbial lifestyle, a nascent multicellular organism, and an incubator for diversity. npj Biofilms Microbiomes 7 (1), 80.
Prata, J.C., da Costa, J.P., Lopes, I., Duarte, A.C., Rocha-Santos, T., 2019. Effects of microplastics on microalgae populations: a critical review. Sci. Total Environ. 665, 400–405.
Quast, C., Pruesse, E., Yilmaz, P., Gerken, J., Schweer, T., Yarza, P., Peplies, J., Gloeckner, F.O., 2013. The SILVA ribosomal RNA gene database project: improved data processing and web-based tools. Nucleic Acids Res. 41 (D1), D590–D596.
Rognes, T, F, T., Nichols, B, Quince, C, Mahé, F, 2016. VSEARCH: a versatile open source tool for metagenomics. PeerJ 4, e2584.
San, K.Y., Bennett, G.N., Berríos-Rivera, S.J., Vadali, R.V., Yang, Y.T., Horton, E., Rudolph, F.B., Sariyar, B., Blackwood, K., 2002. Metabolic engineering through cofactor manipulation and its effects on metabolic flux redistribution in *Escherichia coli*. Metab. Eng. 4 (2), 182–192.

Seeley, M.E., Song, B., Passie, R., Hale, R.C., 2020. Microplastics affect sedimentary microbial communities and nitrogen cycling. Nat. Commun. 11 (1), 2372.
Simon, J., Gross, R., Einsle, O., Kroneck, P.M.H., Kröger, A., Klimmek, O., 2000. A NapC/NirT-type cytochrome c (NrfH) is the mediator between the quinone pool and the cytochrome c nitrite reductase of Wolinella succinogenes. Mol. Microbiol. 35 (3), 686–696.
Simon, M., van Alst, N., Vollertsen, J., 2018. Quantification of microplastic mass and removal rates at wastewater treatment plants applying Focal Plane Array (FPA)-based Fourier Transform Infrared (FT-IR) imaging. Water Res. 142, 1–9.
Su, X., Chen, Y., Wang, Y., Yang, X., He, Q., 2019. Impacts of chlorothalonil on denitrification and N_2O emission in riparian sediments: Microbial metabolism mechanism. Water Res. 148, 188–197.
Su, X., Yang, L., Yang, K., Tang, Y., Wen, T., Wang, Y., Rillig, M.C., Rohe, L., Pan, J., Li, H., Zhu, Y.g., 2022. Estuarine plastisphere as an overlooked source of N_2O production. Nat. Commun. 13 (1), 3884.
Sulistyowati, L., Nurhasanah, Riani, E., Cordova, M.R., 2022. The occurrence and abundance of microplastics in surface water of the midstream and downstream of the Cisadane River, Indonesia. Chemosphere 291, 133071.
Sun, J., Dai, X., Wang, Q., van Loosdrecht, M.C.M., Ni, B.J., 2019. Microplastics in wastewater treatment plants: detection, occurrence and removal. Water Res. 152, 21–37.
Tan, Y., Zhu, X.Y., Wu, D., Song, E.Q., Song, Y., 2020. Compromised autophagic effect of polystyrene nanoplastics mediated by protein corona was recovered after lysosomal degradation of corona. Environ. Sci. Technol. 54 (18), 11485–11493.
Tu, Q., Lin, L., Cheng, L., Deng, Y., He, Z., 2019. NCycDB: a curated integrative database for fast and accurate metagenomic profiling of nitrogen cycling genes. Bioinformatics 35 (6), 1040–1048.
Vymazal, J., Greenway, M., Tonderski, K., Brix, H., Mander, Ü., 2006. Constructed wetlands for wastewater treatment. Wetlands and Natural Resource Management. Springer Berlin Heidelberg, Berlin, Heidelberg, pp. 69–96. Verhoeven, J. T. A.; Beltman, B.; Bobbink, R.; Whigham, D. F., Eds.
Vymazal, J., 2007. Removal of nutrients in various types of constructed wetlands. Sci. Total Environ. 380 (1-3), 48–65.
Wang, C., Wei, W., Zhang, Y.T., Dai, X., Ni, B.J., 2022. Different sizes of polystyrene microplastics induced distinct microbial responses of anaerobic granular sludge. Water Res. 220, 118607.
Wood, D.E., Lu, J., Langmead, B., 2019. Improved metagenomic analysis with Kraken 2. Genome Biol. 20 (1), 257.
Wrage, N., van Groenigen, J.W., Oenema, O., Baggs, E.M., 2005. A novel dual-isotope labelling method for distinguishing between soil sources of N_2O. Rapid Commun. Mass Spectrom. 19 (22), 3298–3306.
Wu, H., Wang, R., Yan, P., Wu, S., Chen, Z., Zhao, Y., Cheng, C., Hu, Z., Zhuang, L., Guo, Z., Xie, H., Zhang, J., 2023. Constructed wetlands for pollution control. Nat. Rev. Earth Environ. 4, 218–234.
Xu, Y., Ou, Q., Wang, X., Hou, F., Li, P., van der Hoek, J.P., Liu, G., 2023. Assessing the mass concentration of microplastics and nanoplastics in wastewater treatment plants by pyrolysis gas chromatography-mass spectrometry. Environ. Sci. Technol. 57 (8), 3114–3123.
Yang, X., Chen, Y., Liu, X., Guo, F., Su, X., He, Q., 2018. Influence of titanium dioxide nanoparticles on functionalities of constructed wetlands for wastewater treatment. Chem. Eng. J. 352, 655–663.
Yang, X., Chen, Y., Guo, F., Liu, X., Su, X., He, Q., 2020. Metagenomic analysis of the biotoxicity of titanium dioxide nanoparticles to microbial nitrogen transformation in constructed wetlands. J. Hazard. Mater. 384, 121376.
Yang, X., He, Q., Guo, F., Sun, X., Zhang, J., Chen, M., Vymazal, J., Chen, Y., 2020. Nanoplastics disturb nitrogen removal in constructed wetlands: responses of microbes and macrophytes. Environ. Sci. Technol. 54 (21), 14007–14016.
Yang, X., He, Q., Liu, T., Zheng, F., Mei, H., Chen, M., Liu, G., Vymazal, J., Chen, Y., 2022. Impact of microplastics on the treatment performance of constructed wetlands: Based on substrate characteristics and microbial activities. Water Res. 217, 118430.
Yang, X., Zhang, L., Chen, Y., He, Q., Liu, T., Zhang, G., Yuan, L., Peng, H., Wang, H., Ju, F., 2022. Micro(nano)plastic size and concentration co-differentiate nitrogen transformation, microbiota dynamics, and assembly patterns in constructed wetlands. Water Res. 220, 118636.
Yarza, P., Yilmaz, P., Pruesse, E., Glöckner, F.O., Ludwig, W., Schleifer, K.H., Whitman, W.B., Euzéby, J., Amann, R., Rosselló-Móra, R., 2014. Uniting the classification of cultured and uncultured bacteria and archaea using 16S rRNA gene sequences. Nat. Rev. Microbiol. 12 (9), 635–645.
Yu, H., Zhang, Z., Zhang, Y., Song, Q., Fan, P., Xi, B., Tan, W., 2021. Effects of microplastics on soil organic carbon and greenhouse gas emissions in the context of straw incorporation: a comparison with different types of soil*. Environ. Pollut. 288, 117733.
Zeng, L., Dai, Y., Zhang, X., Man, Y., Tai, Y., Yang, Y., Tao, R., 2021. Keystone species and niche differentiation promote microbial N, P, and COD removal in pilot scale constructed wetlands treating domestic sewage. Environ. Sci. Technol. 55 (18), 12652–12663.
Zhao, C., Xie, H., Xu, J., Xu, X., Zhang, J., Hu, Z., Liu, C., Liang, S., Wang, Q., Wang, J., 2015. Bacterial community variation and microbial mechanism of triclosan (TCS) removal by constructed wetlands with different types of plants. Sci. Total Environ. 505, 633–639.
Zhou, Y., He, G., Bhagwat, G., Palanisami, T., Yang, Y., Liu, W., Zhang, Q., 2023. Nanoplastics alter ecosystem multifunctionality and may increase global warming potential. Glob. Change Biol. 29 (14), 3895–3909.
Zhu, X.Y., Peng, L., Song, E.Q., Song, Y., 2022. Polystyrene nanoplastics induce neutrophil extracellular traps in mice neutrophils. Chem. Res. Toxicol. 35 (3), 378–382.
Zumft, W.G., 1997. Cell biology and molecular basis of denitrification. Microbiol. Mol. Biol. Rev. 61 (4), 533. -+.